



System Identification - Theory and Practice

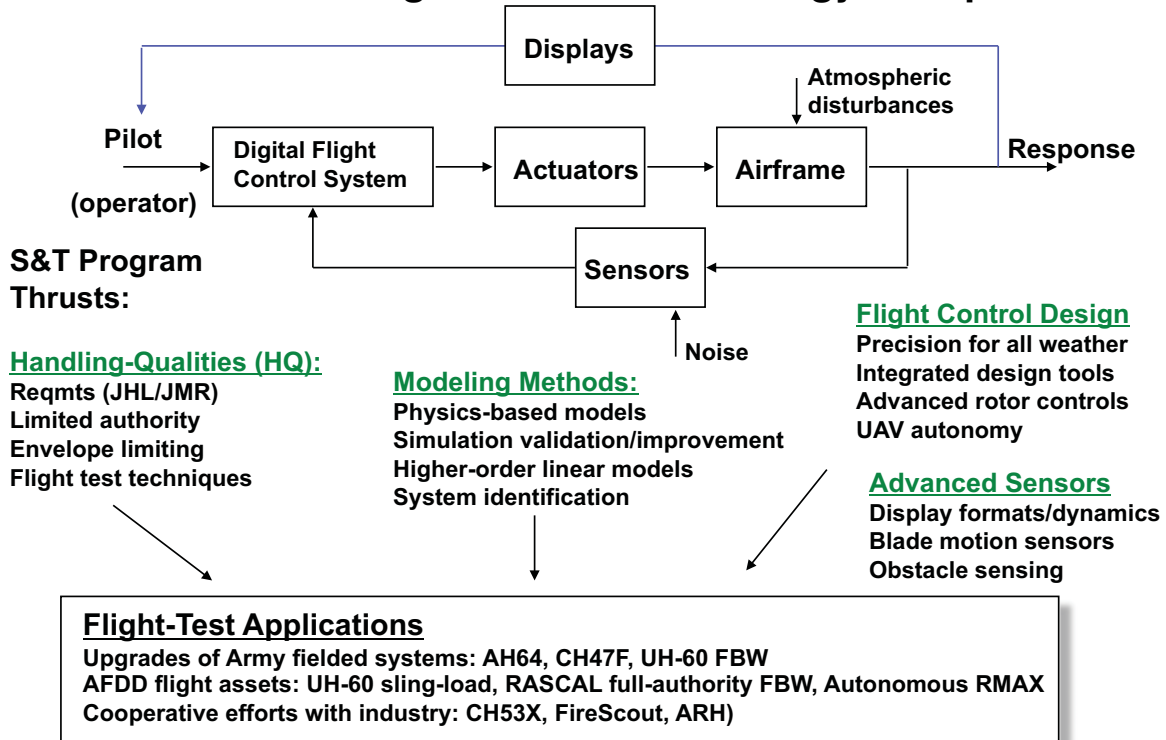
Dr. Mark B. Tischler
Senior Scientist
Us Army Aeroflightdynamics Directorate

Mr. Kenny K. Cheung
Principal Flight Control Software Engineer
University Affiliated Research Center (UARC)
University of California, Santa Cruz

Outline

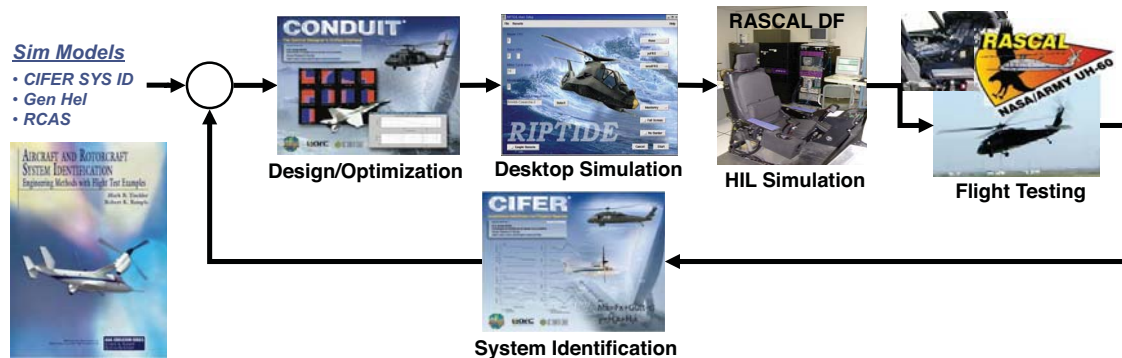
- **AFDD flight control technology group and key design tools**
- **Background on system identification**
- **Key roles for flight simulation and flight control development**
- **Demonstration of CIFER®**
- **Questions**

AFDD Flight Control Technology Group



3

Rapid Desktop-to-Flight Development Pathway



Applications:

- Improved handling qualities of new and current aircraft
- UAV control laws with any level of autonomy or cooperation
- Advanced system control modes (INav&FC) and displays (HMDs)
- Hardware-in-the-loop (HIL) simulation and on-board-monitoring
- Basic launch platform for evaluating advanced concepts

⇒ Successfully applied to CH-47F DAFCS, AH-64D MCLAWS, CH-53X, UH-60M, ARH, Fire Scout, improving accuracy and speed of design

4

AFDD Design Tool Application

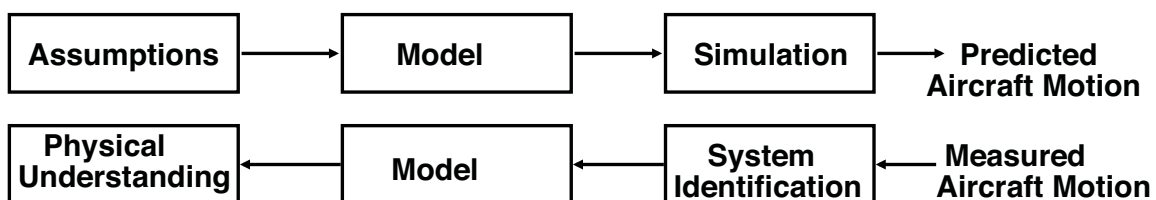


5

Background

- What is aircraft system identification?

- Determination of a mathematical description of aircraft dynamic behavior from measured aircraft motion



- What are system identification results used for?

- Wind tunnel vs. flight test measured characteristics
- Simulation model development / validation
- Subsystem hardware/software modeling
- HQ specification compliance
- Optimization of automatic flight control systems

- What are the special problems that arise in applying system ID to aircraft?

- High level of measurement noise
- High degree of inter-axis coupling
- High order of dynamical system
- Unstable vehicle dynamics

6

Nonparametric and Parametric Modeling

- **Nonparametric modeling: no model structure or order is assumed**
 - frequency-response (frequency-domain)

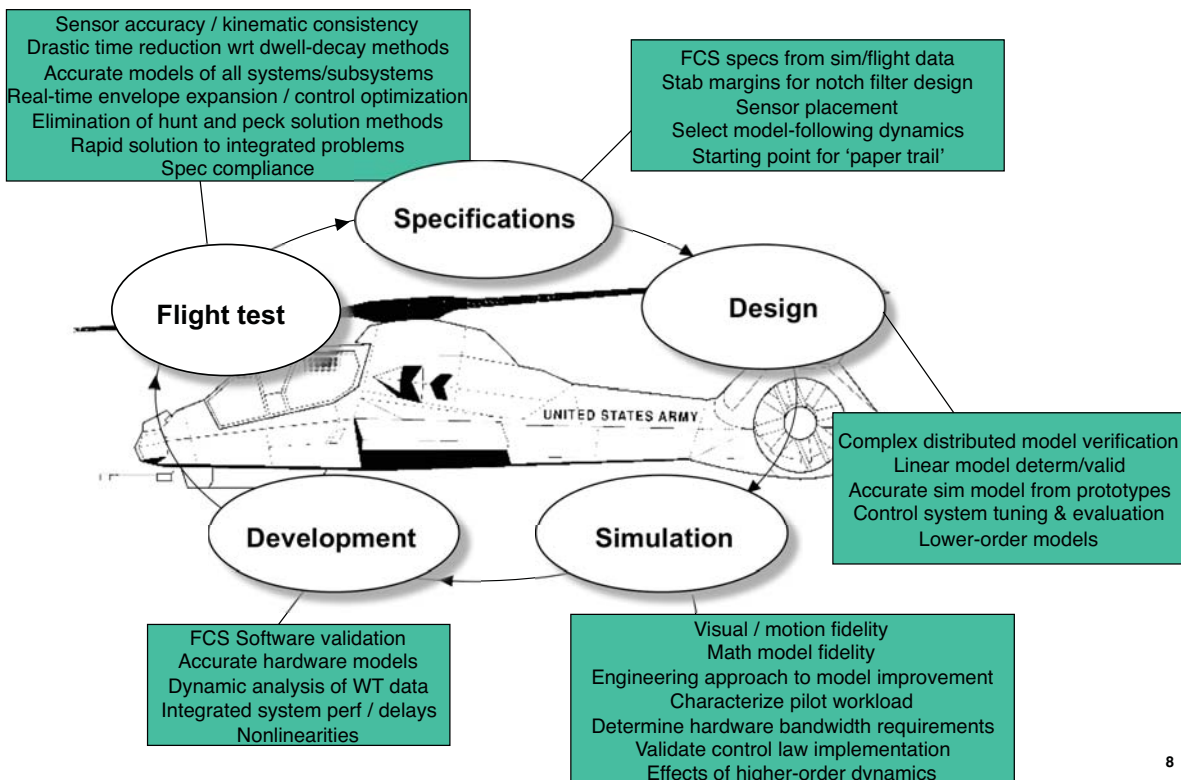
Bode plot format: Log-mag (db) and phase (deg) of input-to-output ratio vs. freq.

Applications: bandwidth, time-delay, pilot-in-the-loop analysis, math model validation, parametric model structure and order
- **Parametric modeling: model order and structure must be assumed**
 - transfer-function: pole-zero representation of individual freq. response pairs
 - state-space description: aerodynamic stability and control derivative representation

Applications: control system design, wind-tunnel and math model validation

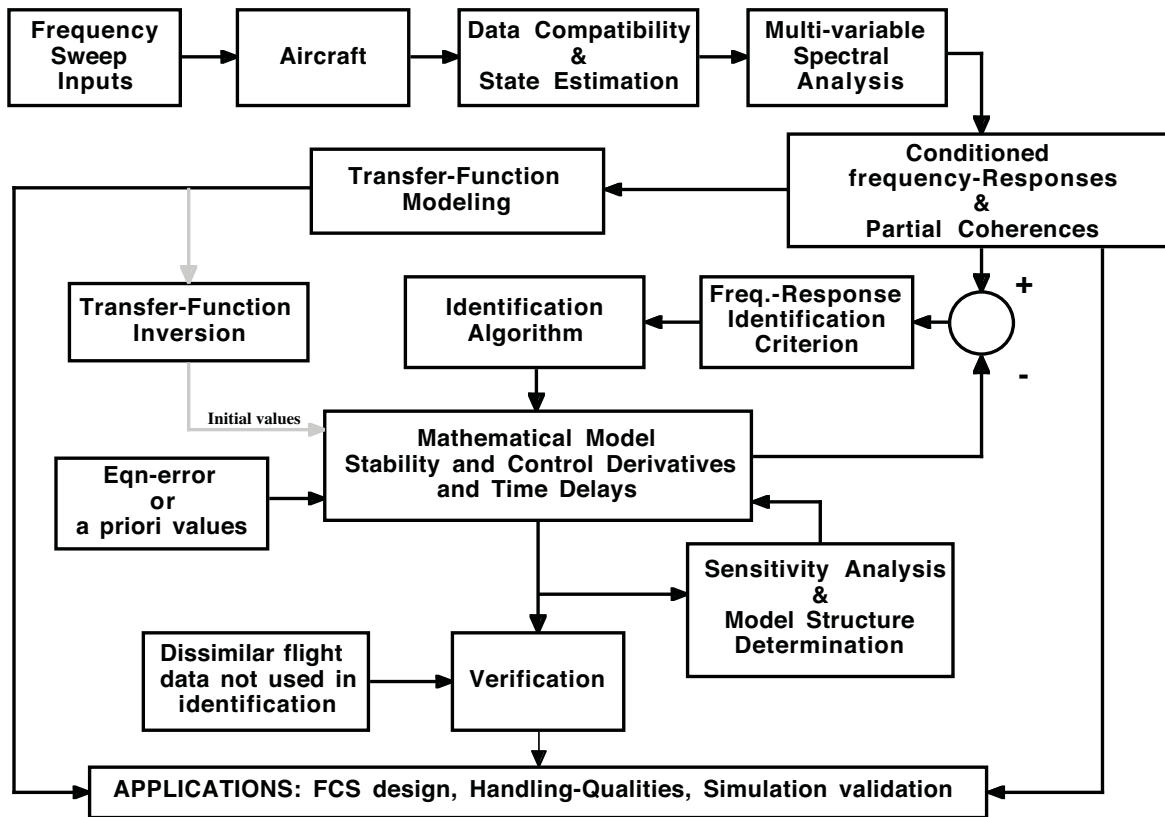
7

How will SID Support the Development Process?



8

Frequency-Response Method for System ID



9

Key Features of Frequency-Response Approach for System Identification

- Frequency-response calculation eliminates uncorrelated process and output measurement noise effects:

$$\text{Frequency-response: } \hat{H} = \frac{G_{xy}}{G_{xx}}$$

- Parametric models are obtained by matching the nonparametric frequency-response in frequency-range where the data is most accurate:

$$\text{Coherence: } \hat{\gamma}_{xy}^2 = \frac{|G_{xy}|^2}{|G_{xx}| |G_{yy}|}$$

- Time delays can be identified directly:

$$\Phi = -\omega \tau$$

10

Frequency-Response Method Features (Cont)

- Number of unknowns greatly reduced relative to time-domain solution

$$\dot{x} = Fx + Gu(t-\tau) + \text{bias}$$

$$y = Hx + ju(t-\tau) + y_{\text{ref}}$$

$$T(s) = (H[sI-F]^{-1}G + j) e^{-\tau s}$$

6 dof model:

number of unknowns in F, G, tau = 64

time-domain soln: 8 bias terms + (9 outputs x 4 records) = 44 extra terms

- Data points in cost function greatly reduced relative to time-domain soln
=> Well suited to identification of coupled rigid body/structural dynamics
- Applicable to identification of unstable systems
=> TD integration errors make this very difficult for long data records.

11

Frequency-Domain SID Methods are Especially Well-Suited to Flight Control System Development and Validation

- Well suited to complex problems:
 - Multiple overlapping modes, unstable systems, low signal-to-noise
- Frequency-responses are nonparametric characterizations obtained without first determining state-space model structure
- Broken-loop & closed-loop responses provide important “paper trail”
- Feedback stability and noise amplification determined from broken-loop frequency-response => crossover freq., gain/phase margins, PSD
- Command tracking based on end-to-end closed-loop response
=> bandwidth, phase delay, and lower-order equiv. systems

Payoffs:

- * HQ/AFCS/Vib testing accounts for 37% of all flight testing

(Ref. Crawford, “Potential for Enhancing the Rotorcraft Development / Qualification Process using System Identification,” RTO SCI Symposium on System Identification for Integrated Aircraft Development and Flight Testing,” 5-7 May 1998, Madrid, Spain.)

- * Modern FBW flight test programs cost approx. \$50K/flight-hr

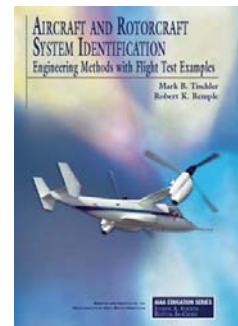
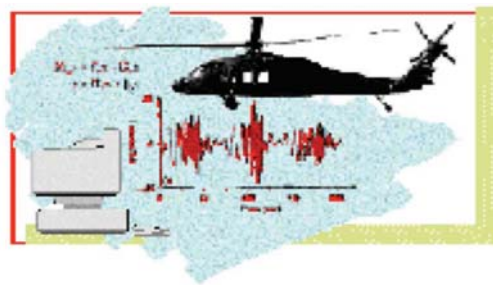
12

CIFER®

Comprehensive Identification from FrEquency Responses

Key features of the CIFER® approach are:

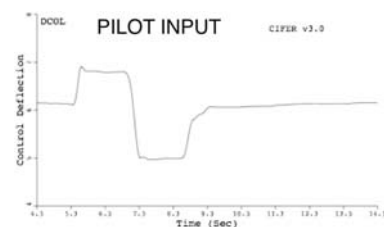
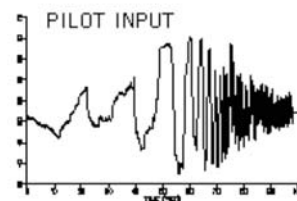
- Integrated databasing and screen-driven commands
- Unique ID and analysis algorithms highly-exercised on many flight projects (r/c and fixed-wing)
- MIMO frequency-response solution
- Highly-flexible and interactive definition of ID model structures.
- Very reliable, systematic, and integrated model structure procedure
- Integrated model verification in the time-domain



13

Frequency-Domain SID Maneuvers

- Identification maneuver: Frequency-Sweep
 - Well suited to freq.-domain SID
 - Even distribution of spectral content
 - Input and output are roughly symmetric
 - Frequency-range is strictly controlled during test
 - Very safe and well established method.
- Verification maneuver: Doublet
 - Characteristic of realistic pilot input
 - Symmetric response keeps aircraft within flight condition used in the SID tests
 - Different form than sweeps - guards against overtuning of identification

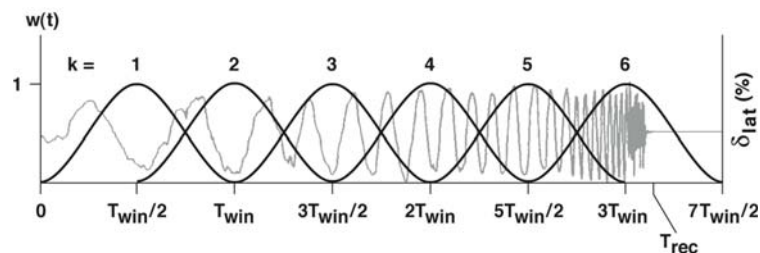


Instrumentation Requirements for Aircraft Application

- **Sample rate:**
 - All signals at same sample rate and filtering
 - Desired rate is 25x modes of interest
 - » 50 hz for rigid body response
 - » 100 hz for structural response to 4 hz
- **Piloted control inputs**
- **Aerosurface deflections**
- **SAS command inputs**
- **Aircraft response:**
 - Alpha, beta
 - p, q, r
 - Phi, theta
 - ax, ay, az
- **Structural response:**
 - Wing tip accelerometers
 - Fuselage accelerometers

15

Overlapped Averaging

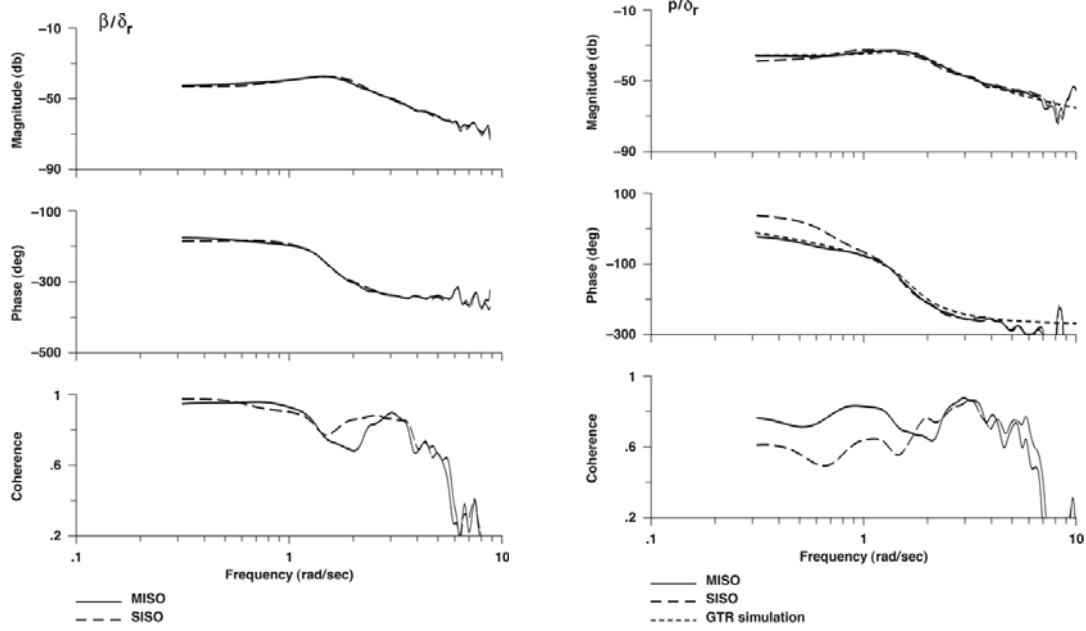


- **Chirp z Transform allows FFT over freq. Range of interest with flexibility and high resolution**
- **Random error is inversely proportional to sqrt of # of windows**

16

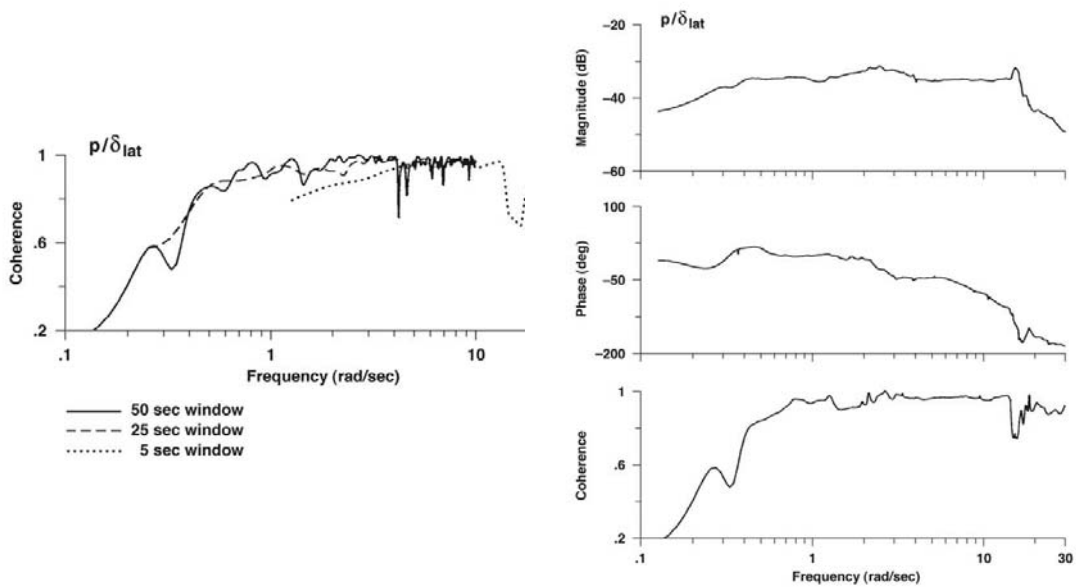
Importance of Multi-Input Solution for Coupled System ID

$$\frac{y_j}{x_i}(f) = \frac{G_{x_i y_j}}{G_{x_i x_i}} \neq G^{-1}_{xx}(f) G_{xy}$$



17

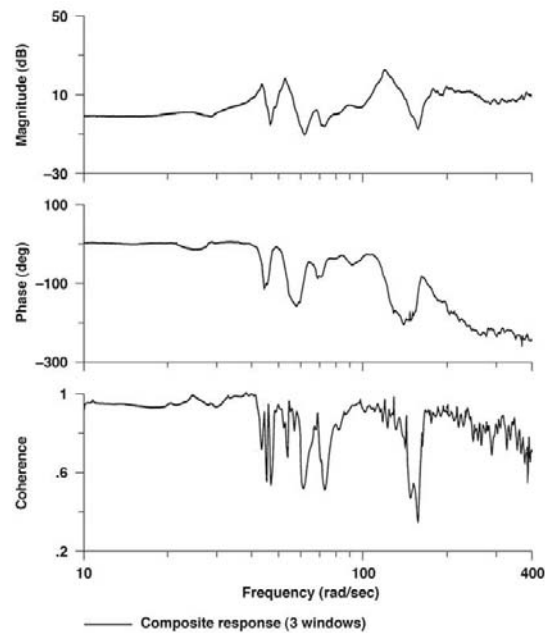
Composite Window Averaging



- Final composite frequency-response ID has exceptional accuracy and dynamic range

18

COMPOSITE Window Especially Important for Structural Response ID



19

Frequency-Response Matching Procedure

- The state-space model is formulated in general as:

$$\begin{aligned} \mathbf{M}_m \dot{\mathbf{x}} &= \mathbf{F}_m \mathbf{x} + \mathbf{G}_m \mathbf{u} \\ \mathbf{y} &= \mathbf{H}_m \mathbf{x} + \mathbf{j}_m \mathbf{u} \end{aligned}$$

The elements of \mathbf{M}_m , \mathbf{F}_m , \mathbf{G}_m , \mathbf{H}_m , \mathbf{j}_m are the unknown s&c derivatives
=> some elements may be known from physical considerations or TF models

- Taking Laplace transform:

$$\mathbf{T}_m(s) = \mathbf{H}_m [s\mathbf{I} - \mathbf{M}_m^{-1} \mathbf{F}_m]^{-1} \mathbf{M}_m^{-1} \mathbf{G}_m + \mathbf{j}_m$$

- Incorporate a matrix of time delay functions $\boldsymbol{\tau}_m(s)$ and eliminate \mathbf{j}_m by allowing \mathbf{H}_m to be a function of s :

$$\mathbf{T}_m(s) = \mathbf{H}_m(s) [s\mathbf{I} - \mathbf{M}_m^{-1} \mathbf{F}_m]^{-1} \mathbf{M}_m^{-1} \mathbf{G}_m \boldsymbol{\tau}_m(s)$$

3b-20

Frequency-Response Cost Function

The unknown parameters (state-space matrices) are determined by minimizing the weighted cost function J :

$$J(\Theta) = \sum_{n=1}^{n_{\omega}} \epsilon^T(\omega_n, \Theta) W \epsilon(\omega_n, \Theta)$$

$\omega_1, \omega_2, \dots, \omega_{n_{\omega}}$: freq. points for each input/output pair; range is selected based on individual range of good coherence and overall applicability of model structure

ϵ : vector of magnitude and phase errors between the identified MISO (composite) frequency-responses $T(s)$ and the model responses $T_m(s)$

W : weighting function at each freq. and for each FR pair; comprised of:

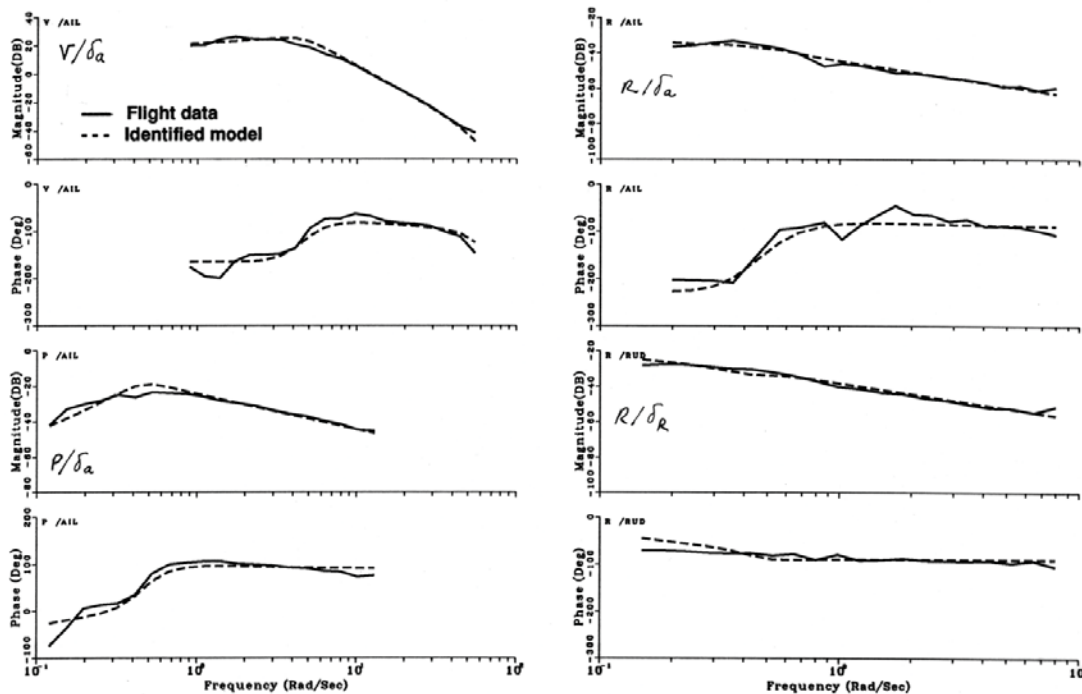
- relative magnitude / phase weighting (nominal: 7.57 deg: 1dB)
- coherence weighting

⇒ Nonlinear minimization using Secant pattern search to find (local) minimum of J

3b-21

Stability and Control Derivative Model ID (Hover)

CIFER v2



3b-22

XV-15 Tilt-Rotor Identification Results (Hover)

$$\dot{\mathbf{x}} = \mathbf{F}\mathbf{x} + \mathbf{G}\mathbf{u}$$

$$\mathbf{y} = \mathbf{H}\mathbf{x} + \mathbf{j}\mathbf{u}$$

F-matrix

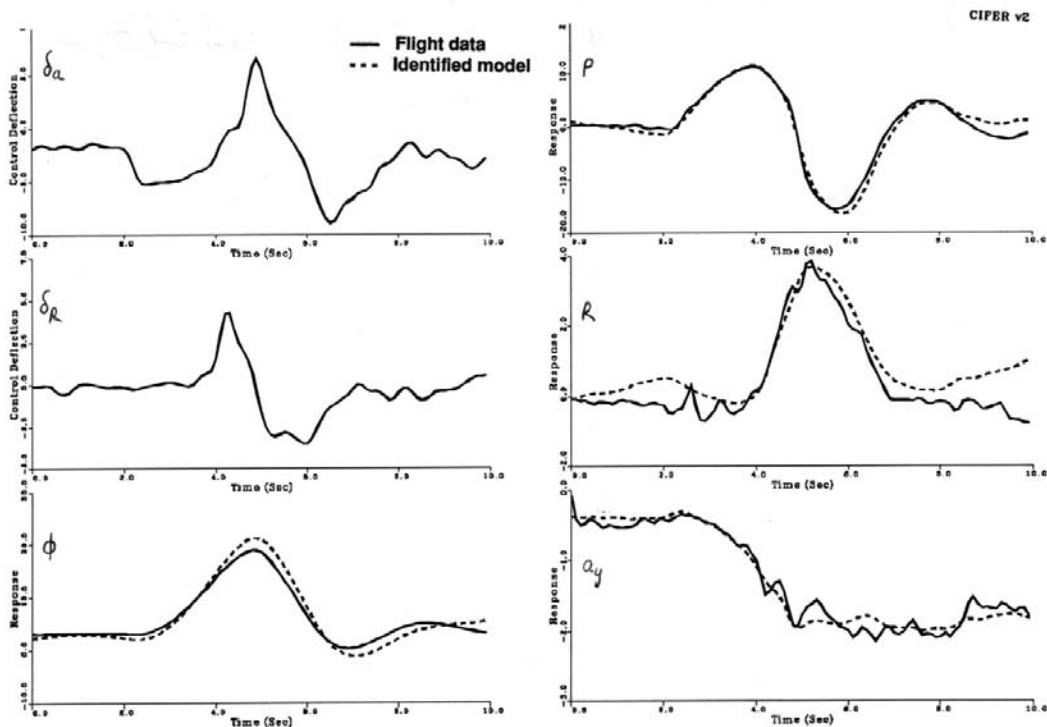
XVMOD4		
Derivative	Param Value	C.R. (%)
Y_v	-0.1102	6.271
Y_p	-1.422	12.46
Y_r	0.000 +
G	32.17 †
L_v	-3.775E-03	6.084
L_p	-0.2775	15.64
L_r	-0.8726	13.17
N_v	6.337E-04	7.425
N_p	0.02914	30.20
N_r	0.000 +
K_{in}	1.000 †

G-matrix

XVMOD4		
Derivative	Param Value	C.R. (%)
Y_{δ_a}	-0.04584	5.925
Y_{δ_r}	0.000 +
L_{δ_a}	-0.06094	3.039
L_{δ_r}	0.000 +
N_{δ_a}	5.909E-03	4.802
N_{δ_r}	0.01238	4.650
τ_{ail}	0.000
τ_{rud}	0.000

+ Eliminated during model structure determination

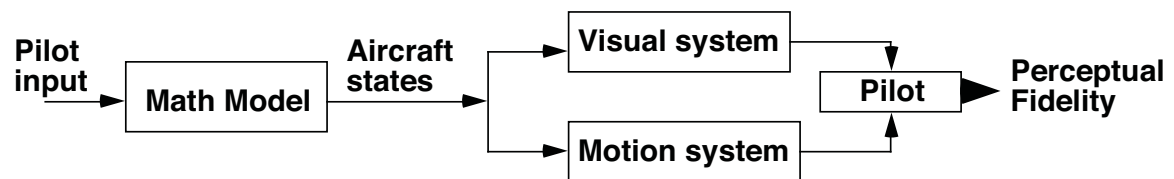
Verification of State-Space Model (Hover)



Key Roles of CIPHER System ID for Flight Simulation

25

Simulation Components

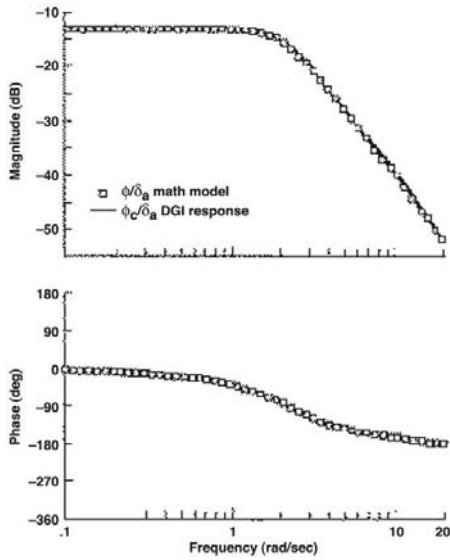


=> Perceptual fidelity: end-to-end frequency response

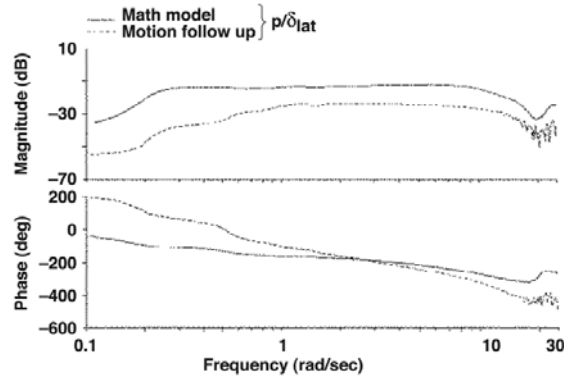
26

Validation of Simulator Visual and Motion Systems (VMS, Ames)

Visual System Response Includes McFarland Compensation



Motion System Response



27

Component Type Model (GenHel)

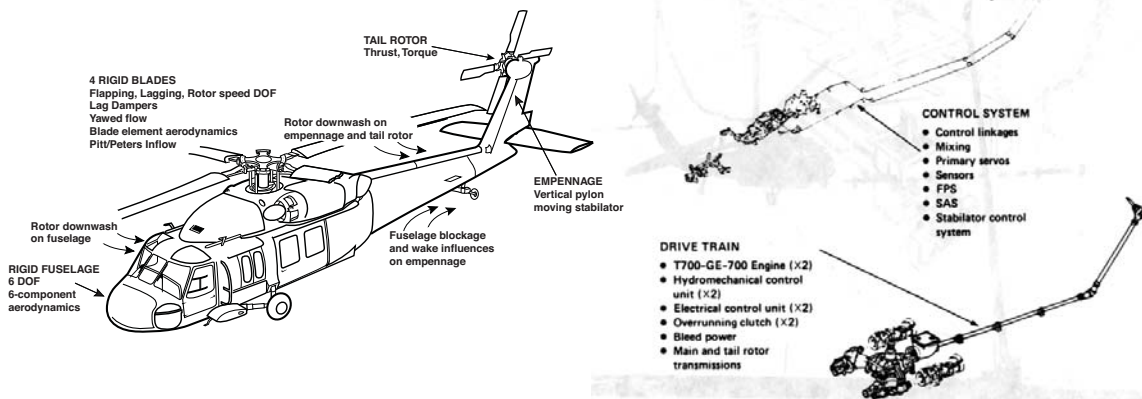


Fig. 1. Sikorsky-Ames Gen Hel UH-60 real-time simulation model.

28



Verification of Simulation Dynamics

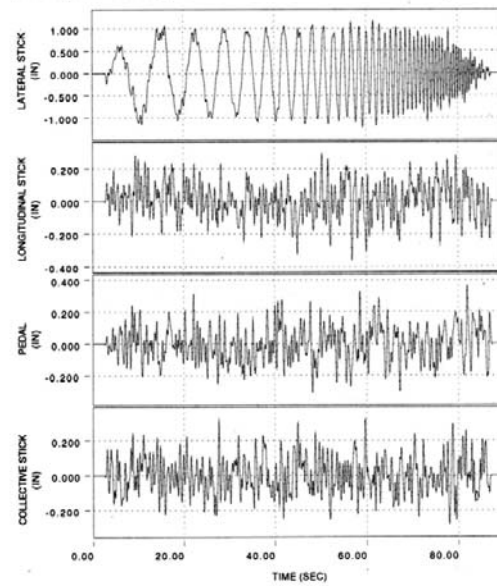
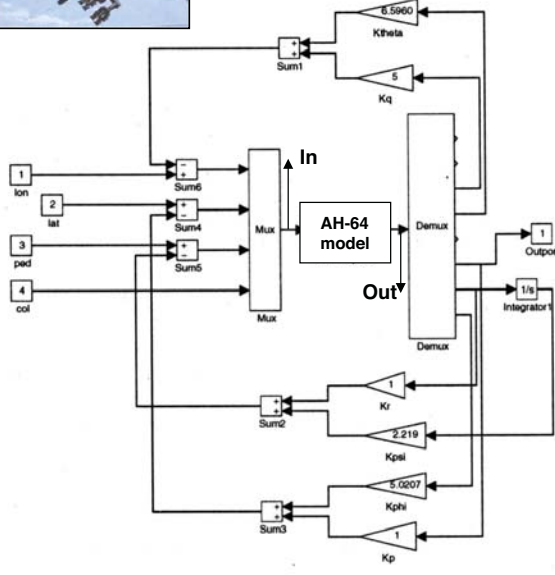
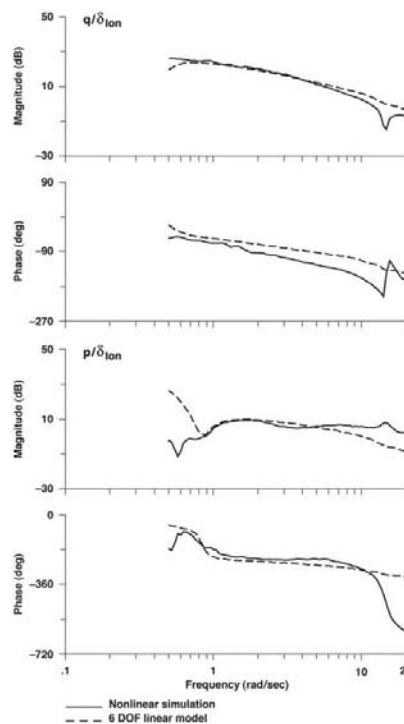


Figure 3: Feedback loops to maintain attitude during frequency sweep

Figure 2: Typical computer generated frequency sweep input including white noise

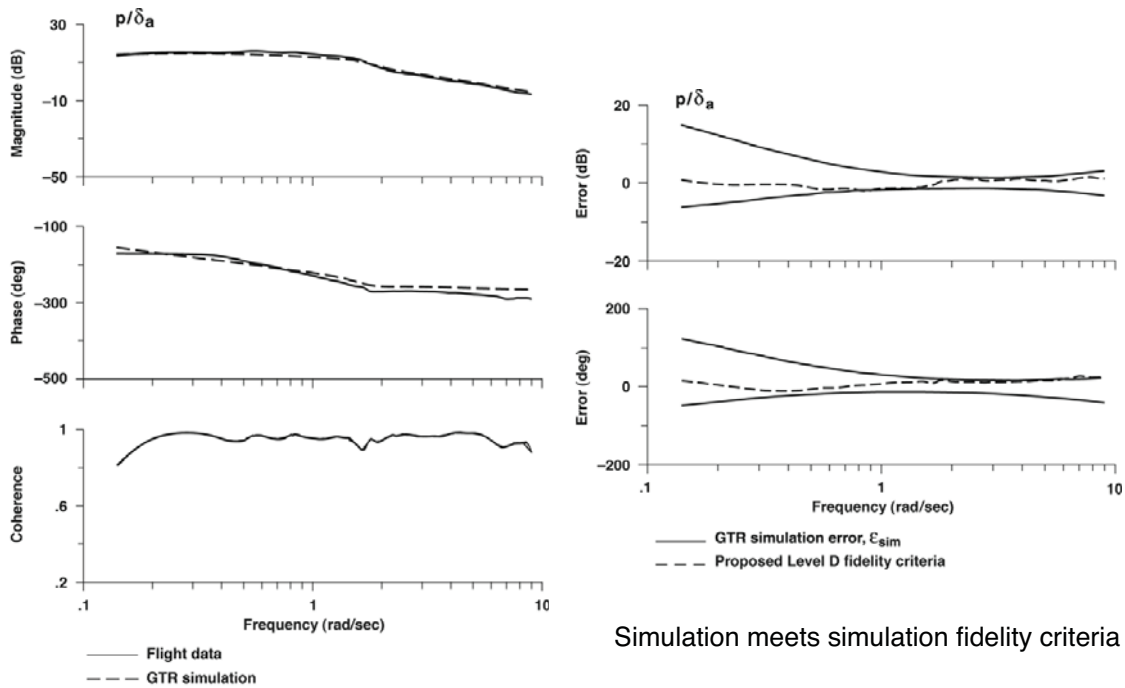
Ref: H. Mansur and M. Tischler, "An Empirical Correction Method for Improving Off-Axis Response in Flight Mechanics Helicopter Models," AHS Journal Vol 43, No. 2, April 1998.

Comparison of Higher-Order Nonlinear Response with 6DOF Perturbation (LINMOD) Model



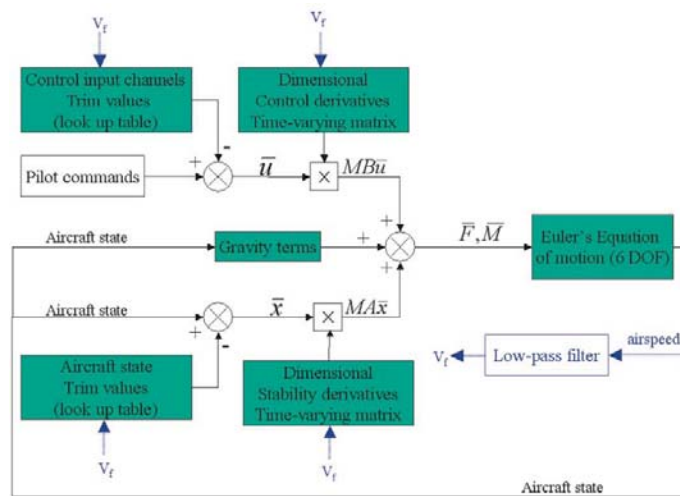
Excellent means to validate distributed model dynamics and linearization methods

Simulation Model Fidelity Assessment (XV-15 cruise)



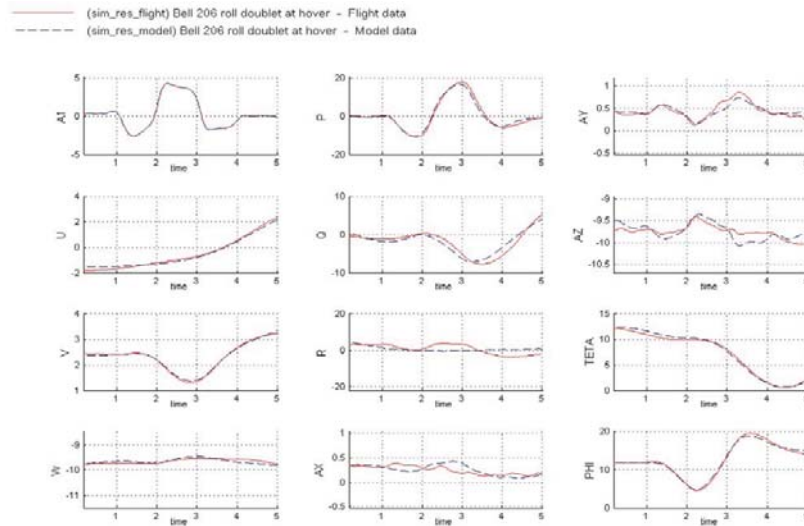
31

Block Diagram for Full Envelope Simulation Model from ID Results (IAI Bell 206)



32

Full Envelope Simulation Model from ID Results (IAI Bell 206)

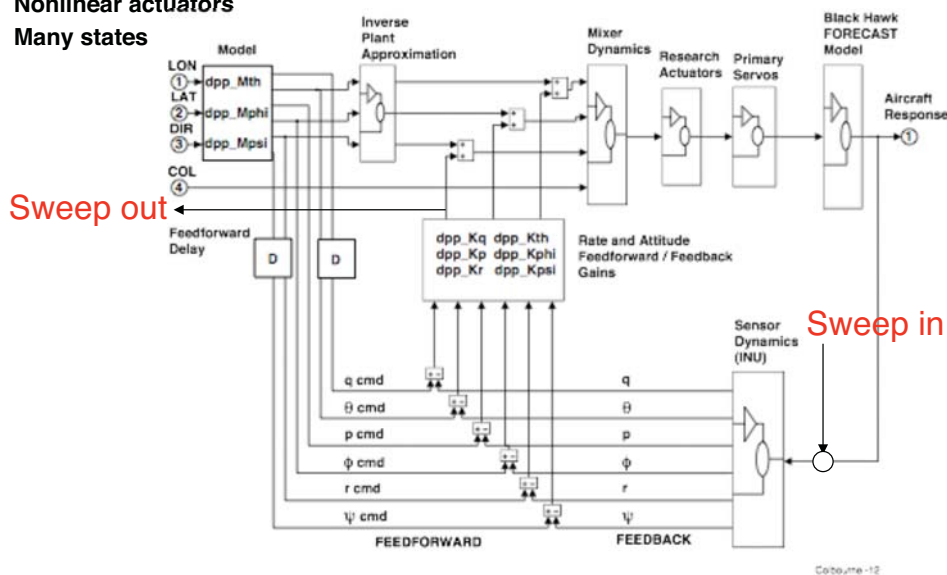


- Efficient and very accurate approach to developing piloted/engineering sim

33

Simulink Model Validation

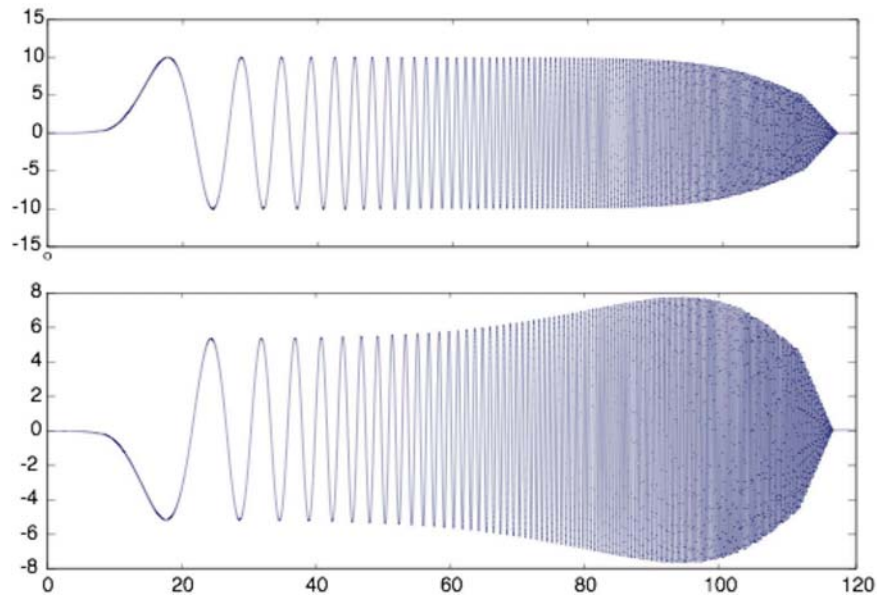
- Full RASCAL control laws
- Nonlinear actuators
- Many states



Extraction of linearized (perturbation) model from SIMULINK model using "LINMOD" function is often inaccurate
=> control system design will not respond as expect in flight.

34

Computer Generated Sweep



35

Validation of SAS Implementation and Linmod

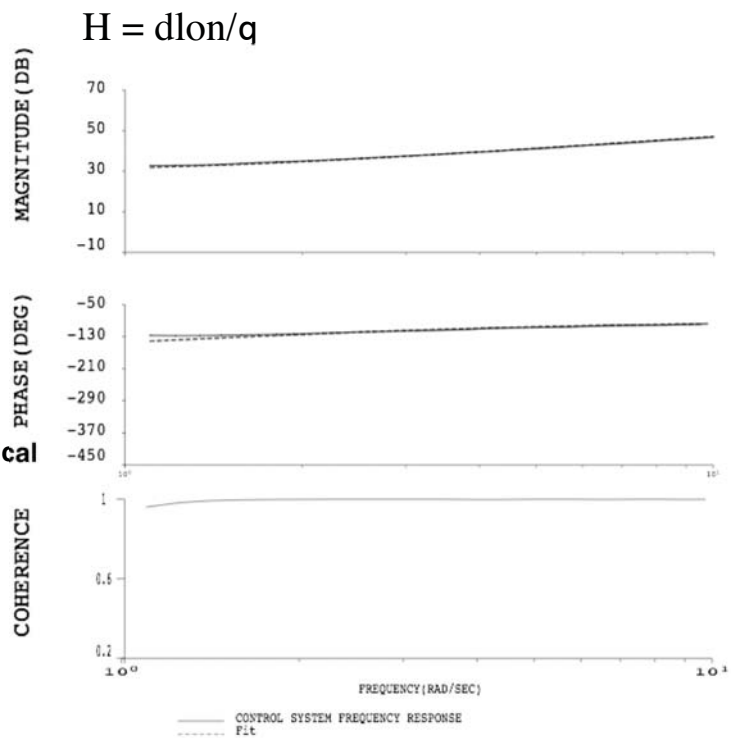
- **Transfer-Function Fit:**

$$\begin{aligned} H_q &= -22.5 (s+1.37) \\ &= -22.5 s - 30.8 \\ &= -K_q s - K_q \end{aligned}$$

- **Analytical gains:**

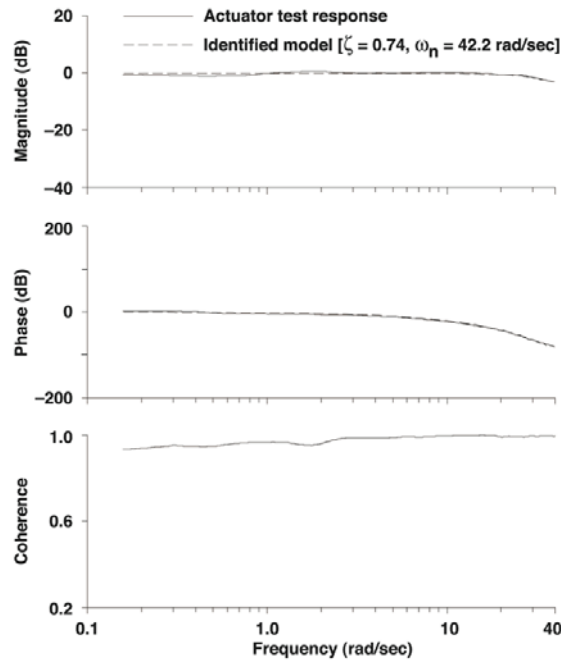
$$\begin{aligned} K_q &= 21.5 \quad (4\%) \\ K_q &= 32.8 \quad (7\%) \end{aligned}$$

- **Small differences due to numerical integration and nonlinearities**



36

Actuator Response Determination from Bench Tests

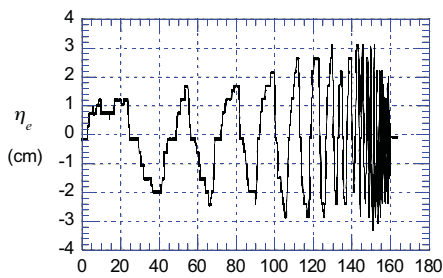


Tschler-18

37

Closed-Loop Handling-Qualities -- TU 144 (M=1.9)

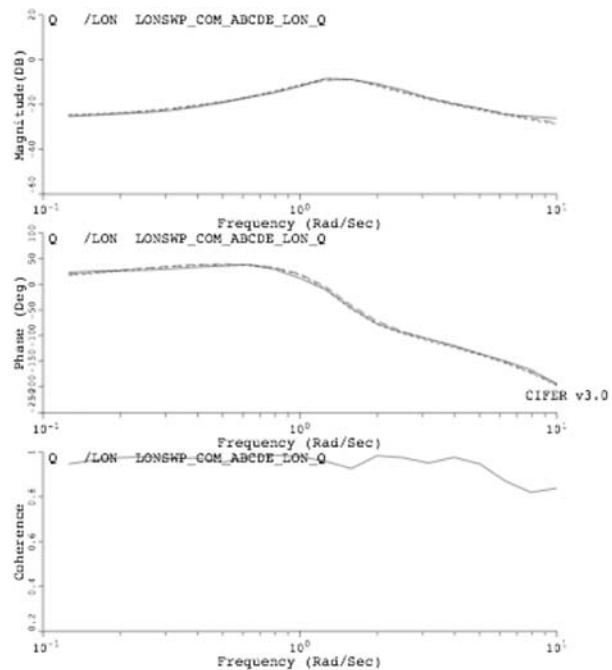
Piloted frequency-sweeps



- LOED Short period dynamics:

$$\frac{q}{\delta_c} = \frac{K_\theta (1/T_{\theta_2}) e^{-\tau_\theta s}}{[\zeta_{sp}, \omega_{sp}]}$$

Excellent agreement of LOES models (OE and CIFER) with frequency response data



LOES Results From Sweep (M=1.9)

Parameter	EE/OE Estimate (Std. Error)	CIFER Estimate (% error)
b_1	0.353 (0.011)	0.380 (5.8%)
b_0	0.106 (0.006)	0.1072 (12.32%)
a_1	0.932 (0.035)	1.040 (11.61%)
a_0	1.970 (0.035)	2.103 (6.3%)
τ_e	0.194 (0.014)	0.192 (6.9%)
$1/\tau_{\theta_2}$	0.30	0.28
ζ_{SP}	0.33	0.36
ω_{SP}	1.40	1.45

Excellent agreement of results for two ID approaches (OE and CIFER) for this simple (rigid body) model

HQ Parameters

$$\zeta_{sp} = 0.36$$

$$\omega_{sp} = 1.45 \text{ r/s}$$

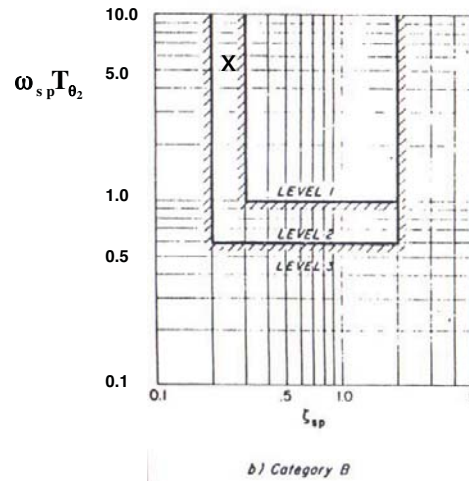
$$\omega_{sp} T_{\theta_2} = 5.18 \text{ rad}$$

Time Delay Limits

- Level 1: $t < 0.10$
- Level 2: $t < 0.20$
- Level 3: $t < 0.30$

=> Level 2 handling-qualities

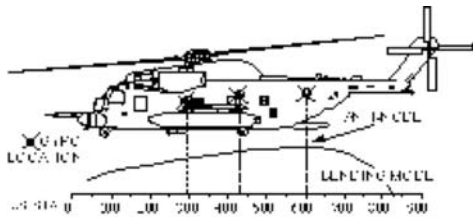
Cat B (gradual maneuvering)



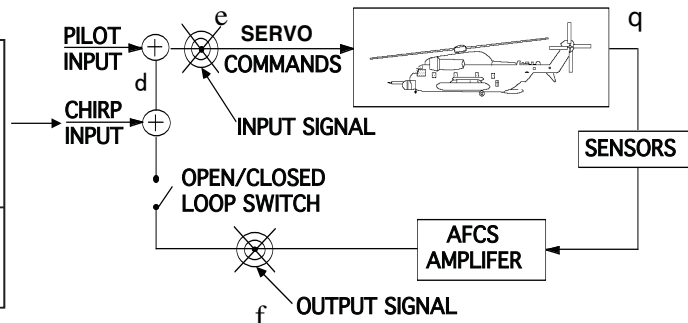
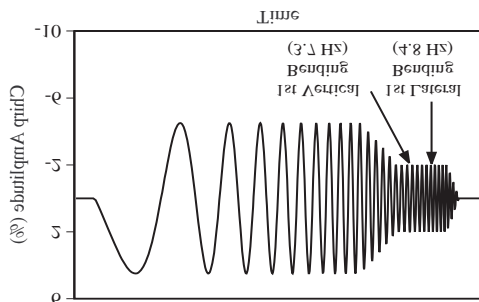
Ref: E. A. Morelli, AIAA-2000-3902, AFM, Aug, 2000, Denver, Co.

MH53J Servo-Elastic Test Program

Sensor locations

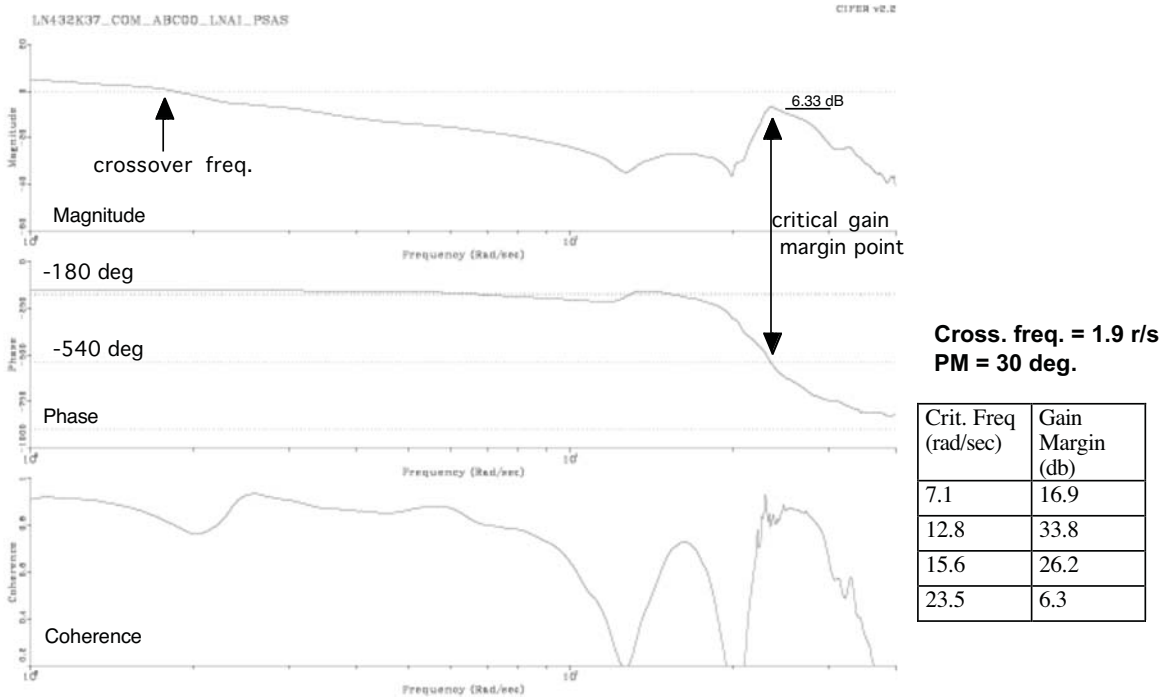


- Stability margin: direct calculation: $f(s) / e(s)$
- Handling-qualities: $(1/s)[q(s)/d(s)]$



Ref: Crawford, "Potential for Enhancing the Rotorcraft Development / Qualification Process using System Identification," RTO SCI Symposium on System Identification for Integrated Aircraft Development and Flight Testing," 5-7 May 1998, Madrid, Spain.

MH53J Stability Margin Results



41

XV-15 Flutter Envelope Clearance Testing



68

C. W. ACREE JR. AND M. B. TISCHLER

J. AIRCRAFT

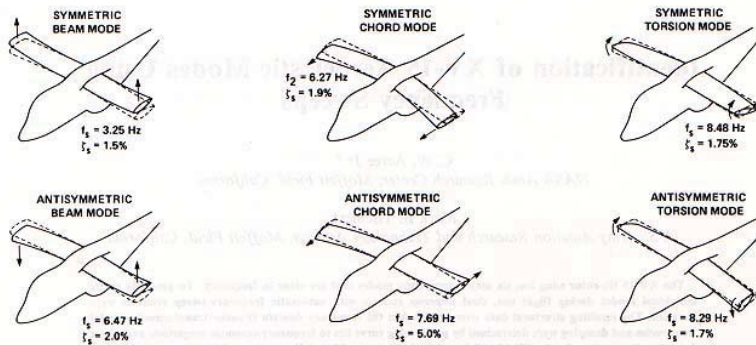


Fig. 2 XV-15 wing modes, with structural frequencies and damping.

42

Modal Identification

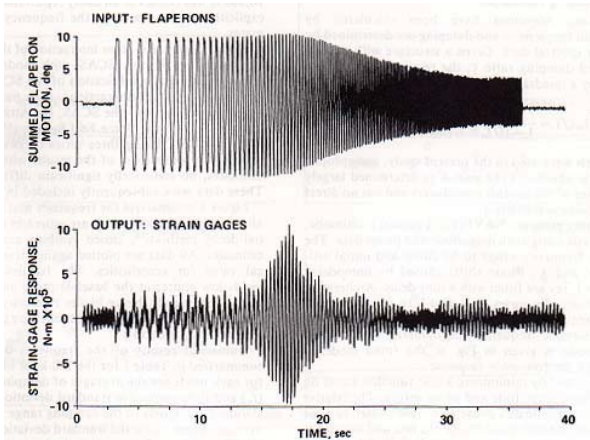


Fig. 5 Input and output time histories for one symmetric flaperon sweep (beam mode).

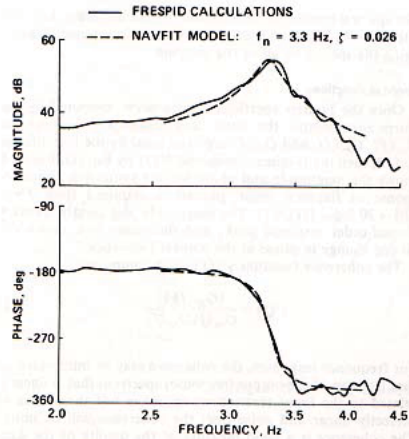
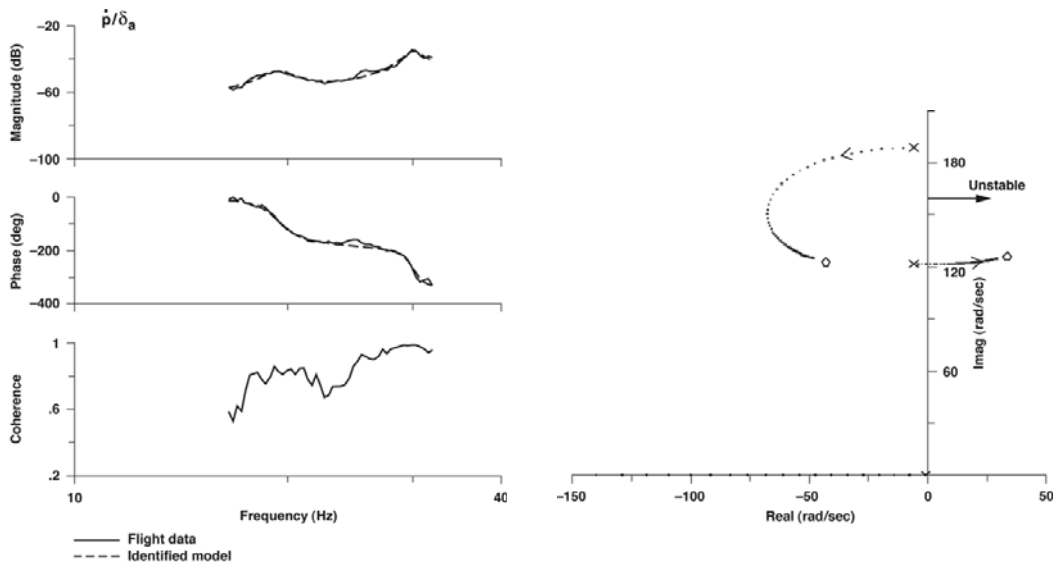


Fig. 6 Symmetric beam mode frequency response and fitted second-order model.

•Sum and difference processing of symmetric measurements significantly improves signal/noise

43

Coupled Rigid Body/Structural ID (AV-8B Harrier)



$$\frac{p}{\delta_a} = \frac{L_{\delta_a}}{(s - L_p)} + \frac{K_1 s}{[s^2 + 2\zeta_1 \omega_{n_1} s + \omega_{n_1}^2]} + \frac{K_2 s}{[s^2 + 2\zeta_2 \omega_{n_2} s + \omega_{n_2}^2]} + \dots$$

$$[\zeta_1 = 0.049; \omega_{n_1} = 19.4 \text{ Hz}] \quad [\zeta_2 = 0.031; \omega_{n_2} = 30.1 \text{ Hz}]$$

44

